Available online at www.sciencedirect.com
SCIENCE DIRECT®
Surface Science 553 (2004) 50–60
SURFACE SCIENCE
www.elsevier.com/locate/susc

Silver on Pt(1 0 0)—room temperature growth and high temperature alloying

Matthias Batzill [1], Bruce E. Koel *

Department of Chemistry, University of Southern California, Los Angeles, CA 90089-0482, USA

Received 3 December 2003; accepted for publication 4 December 2003

Abstract

Growth of submonolayer to monolayer silver films on the reconstructed Pt(1 0 0) surface at 300 K and evolution of the structure with increasing temperature was studied primarily by scanning tunneling microscopy (STM) and Auger electron spectroscopy (AES). At 300 K, formation of elongated 2D-adislands with a composition of $Ag_{80}Pt_{20}$ was observed. This island stoichiometry is dictated by the amount of Pt expelled due to removal of the hex-reconstruction of the clean Pt(1 0 0) surface by the growing Ag adislands. The island shape can be explained by an anisotropic stability of the reconstruction, with the row pattern of the reconstruction acting as a template for island growth. Annealing of the sample above 600 K causes more extensive alloying starting at the perimeter of the Ag adislands by Ag–Pt exchange and formation of a nanophasic Ag–Pt alloy confined to the surface layer. With sufficient Ag, this alloy spreads across the surface until a uniform stoichiometry is established over the entire surface. Temperature-dependent AES studies indicate that there is some mixing of Ag with bulk Pt at elevated temperatures.

Keywords: Auger electron spectroscopy; Scanning tunneling microscopy; Diffusion and migration; Growth; Platinum; Silver; Low index single crystal surfaces; Metal–metal interfaces

1. Introduction

Heteroepitaxy of metals and alloying of metals at interfaces is of continuing interest for both fundamental studies and applications that involve multielement, structured materials. Applications, and model systems for future applications, include multilayer superlattices and ultrathin metal films. These systems often have altered electronic and chemical properties compared to bulk materials. The atomic structure of such multicomponent interfaces will become even more important in the future with the increasing miniaturization of devices and other advances from nanotechnology that will involve atomic-scale structures and their interfaces with different materials.

Here we report on studies of the growth of silver on a Pt(1 0 0) surface. Pt belongs to a family of elements, together with Au and Ir, that exhibit a pseudohexagonal overlayer reconstruction of their clean (1 0 0) surfaces [1–3]. We denote this reconstruction as the 'hex'-reconstruction in the

* Corresponding author. Tel.: +1-213-740-4126; fax: +1-213-740-3972.
E-mail address: koel@chem1.usc.edu (B.E. Koel).
[1] Present address: Department of Physics, Tulane University, New Orleans, LA 70118, USA.

0039-6028/$ - see front matter © 2003 Elsevier B.V. All rights reserved.
doi:10.1016/j.susc.2003.12.023

remainder of this article. The hexagonal overlayer on the square (1 0 0) lattice results in a large unit cell that is apparent in scanning tunneling microscopy (STM) images as a height modulation due to occupation of different sites on the square 'substrate' lattice by atoms in the overlayer. The characteristic structures of this reconstruction are rows with a periodicity of 5 substrate–atom separations along the ⟨0 1 1⟩ direction. The 'troughs' of these rows are due to surface atoms occupying sites on the square lattice close to fourfold hollows, while the 'ridges' of these rows are from atoms that occupy atop sites on the square lattice. Although, some atoms obviously occupy energetically unfavorable positions, formation of the hex-reconstruction reduces the energy by 17% compared to a bulk-truncated (1 0 0)-(1 × 1) surface [4].

STM studies of metal growth on these (1 0 0) surfaces are fairly rare. Examples of such experiments, include homoepitaxial growth on Au [5,6] and Pt [7], and the growth of Sm [8], Re [9], Ge [10], and Au [11] on Pt(1 0 0) and Cu on Ir(1 0 0) [12]. Elongated islands were formed in homoepitaxial growth that could be explained by anisotropic adatom diffusion that results from the row structure of the hex-reconstruction. Deposition of heteroatoms on Pt(1 0 0) also resulted in elongated island structures. For the growth of Sm on Pt(1 0 0), two mechanisms were proposed to lead to elongated island shapes: anisotropic adatom diffusion and preferential lifting of the reconstruction along the 'ridges' of the hex-reconstruction [8].

Adsorption of any of several adsorbates (e.g., $CO_{(a)}$ and $O_{(a)}$) on the Pt(1 0 0)-hex surface has also been observed to lift the reconstruction. STM studies of CO adsorption revealed that lifting of the reconstruction proceeds in a strongly anisotropic manner [13]. Once an unreconstructed region is nucleated at an individual row, removal of the reconstruction proceeds fast along this row. Growth of the unreconstructed domains normal to the rows of the hex-reconstruction, on the other hand, is much slower. This results in a ''row-by-row'' removal of the reconstruction. Molecular beam experiments have determined that 4–5 CO molecules are necessary to nucleate lifting of the Pt(1 0 0)-hex-reconstruction [14].

Growth of Ag on Pt(1 1 1) has been studied extensively both at low and high temperatures. Nucleation and initial island growth processes were investigated for this system at low temperatures [15]. Deposition of submonolayer amounts of silver and subsequent annealing to above 620 K forms an intermixed Ag–Pt surface with nanometer-sized silver agglomerates embedded in a Pt matrix, or vice versa, depending on the Ag coverage [16–18]. It was proposed that alloying of Ag with Pt reduces stress in pseudomorphic Ag layers and thus alloy formation is a means for reducing the free energy of the system. Tersoff [19] generalized the importance of stress in adlayers to explain surface alloying of elements that are immiscible in the bulk. Experimentally, it was found that the intermixed Ag–Pt(1 1 1) alloy was confined to the topmost layer, with no Ag diffusion into the bulk of the Pt crystal. This and the clustering of Ag and Pt in the intermixed surface layer was explained by a positive exchange energy $\varepsilon = \varepsilon_{AgPt} - \frac{1}{2}(\varepsilon_{AgAg} + \varepsilon_{PtPt})$ (with negative ε values). Thus, the observed structure of Ag clusters in a Pt matrix is a result of strain minimization that favors dissolution of Ag in the surface layer and a positive exchange energy that favors Ag–Ag bonds.

In brief communications, we have described the mixing of Ag and Pt at 300 K as a result of lifting of the Pt(1 0 0)-hex-reconstruction by the growing Ag adlayer and the formation of a disordered $Ag_{80}Pt_{20}$ alloy [20] and the coexistence of an Ag–Pt surface alloy with a pure-Pt hex-reconstructed phase in thermodynamic equilibrium for Ag coverages below 0.3 ML [21]. In this article, we present additional studies of the evolution of the surface at different annealing temperatures. Auger electron spectroscopy (AES) studies indicate a reversible mixing of Ag with Pt at elevated temperatures. We also extend our discussion of the growth of Ag on Pt(1 0 0) at 300 K and propose a mechanism for the strongly anisotropic island growth. This mechanism involves an anisotropic stability of the hex-reconstruction and thus is a unique aspect of growth on reconstructed surfaces. We propose that this mechanism for the formation of elongated adislands may allow the use of such reconstructed surfaces as templates to grow nanostructured surfaces by alternating deposition

of two materials that consequently form striped adislands.

2. Experimental methods

Experiments were performed in an UHV chamber that was equipped with a cylindrical mirror analyzer (CMA) for AES, rear-view low energy electron diffraction (LEED) optics, a quadrupole mass spectrometer for residual gas analysis and temperature programmed desorption (TPD), homebuilt single-piezo-tube STM, ion-gun for sample cleaning, resistively heated Ag-evaporation source, and precision-leak valves for gas dosing [22]. For AES, the CMA and its coaxial electron gun were positioned normal to the sample surface. The spectra were recorded in $dN(E)/dE$ mode using a lock-in amplifier and a modulation voltage of 6-V peak-to-peak. To obtain the temperature-dependent AES data, we continuously scanned the Ag double-peak at 351 and 356 eV while the temperature was ramped or kept constant at a preselected value. The peak-to-peak AES-signal (of the entire double-peak energy region) and the temperature were monitored simultaneously. The sample was grounded during AES and the sample was heated radiatively by a filament mounted close to the backside of the crystal. The sample could also be biased and heated by electron bombardment to allow for more efficient heating during sample cleaning and preparation. The sample temperature was measured by a chromel/alumel thermocouple that was spotwelded to the side of the crystal.

The Pt(1 0 0) single crystal was cleaned by standard procedures consisting of cycles of 500-eV Ar^+-ion sputtering and annealing to 1200 K followed by annealing at 1000 K in 5×10^{-7}-Torr O_2 to remove carbon, and finally, annealing to 1200 K in vacuum. The cleanliness of the sample was monitored by AES and the procedure was repeated until no contamination at the surface could be detected. The Ag-evaporation rate was calibrated by AES "uptake plots" on samples that were annealed to 800 K following each deposition cycle in which AES signals were recorded as a function of the Ag-deposition time. Under these conditions, i.e., after annealing to 800 K, Ag and Pt form a surface alloy confined to the topmost layer only. With increasing Ag content, Pt is replaced by Ag in the surface layer until a complete pseudomorphic Ag layer forms [20]. Upon completion of this Ag layer, a "break" or change in slope occurs in the AES uptake plot. The amount of Ag deposited at this break is defined as 1-ML Ag. From the AES uptake plot we determined a deposition rate of 0.004 ML/s, which was kept constant for all experiments. After every Ag deposition, we confirmed the Ag coverage by AES.

3. Results

The morphology of the surface following Ag deposition on a Pt(1 0 0)-hex substrate is described and discussed below. In Section 3.1, we describe the structure that evolves upon silver deposition at 300–400 K. As the sample is annealed to higher temperatures, the surface evolves from a kinetically trapped structure to the thermodynamic equilibrium structure dictated by energy minimization. This is described in Section 3.2 both by STM studies after re-cooling of the sample to 300 K as well as temperature-dependent AES studies that reveal variations in the Ag concentration close to the surface.

3.1. Room temperature growth

STM images after the deposition of submonolayer amounts of Ag on the Pt(1 0 0)-hex surface reveal extended 2D islands, as shown in Fig. 1. These islands are separated by the hex-reconstructed Pt substrate. The islands show strong anisotropic shapes with an elongation along the rows of the hex-reconstruction. Island edges are very straight over several 100 nm and run along the rows of the reconstruction. Furthermore, it appears that the islands preferentially terminate along the 'troughs' of the reconstruction. STM images on top of the islands, as shown in Fig. 1(b), exhibit corrugations of $\sim$0.05 nm. This is significantly less than the atomic step height and can be attributed to incorporated Pt atoms in a Ag matrix [16]. Pt atoms are expelled from the topmost Pt

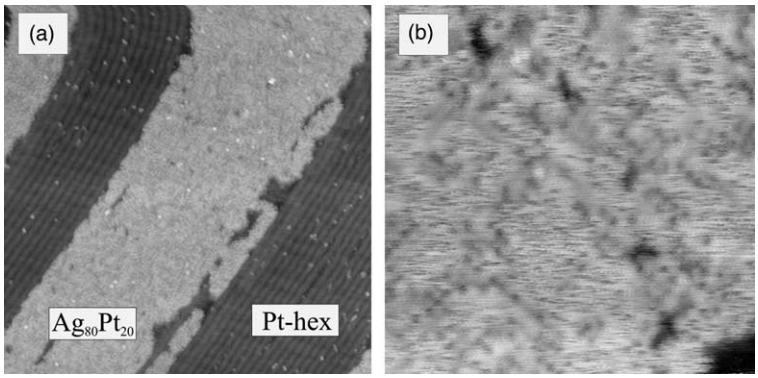

Fig. 1. STM images of submonolayer $Ag_{80}Pt_{20}$ adislands on Pt(1 0 0) after Ag deposition at 300 K. (a) Scan area (60 nm)^2. The adislands exhibit straight edges and are separated from each other by the hex-reconstructed Pt(1 0 0) substrate. (b) Scan area (15 nm)^2. Ag is imaged brighter than Pt. This island shows a disordered structure with 20% Pt dispersed in 80% Ag.

layer when the hex-reconstruction is lifted because the hex-reconstructed surface is more densely packed than the ideal termination of a bulk (1 0 0) layer. As a result, the 'released' Pt atoms combine with Ag adatoms to form 2D islands. Since the hex-reconstructed layer contains 20–25% more Pt atoms than the (1 0 0) layer, a stoichiometry of approximately $Ag_{80}Pt_{20}$ is expected for the 2D adislands. This is in good agreement with STM images if one assumes that Pt is imaged darker. Pt appearing darker in STM compared to Ag has also been observed for Pt–Ag surface alloys on the Pt(1 1 1) surface [16]. This observed chemical contrast between Pt and Ag can partly be explained by the different atomic sizes of the two elements but must mainly be ascribed to electronic effects.

We can construct the scenario that is displayed schematically in Fig. 2 from the STM data. At room temperature, nucleation of adislands on the Pt(1 0 0)-hex surface proceeds by lifting of the hex-reconstruction. This provides additional Pt that is incorporated into the growing islands to form a disordered alloy with a composition close to $Pt_{20}Ag_{80}$. The anisotropic island shape indicates island growth that is faster along the rows of the reconstruction than normal to them. In principle, strongly anisotropic adatom diffusion on the reconstructed surface, as was observed for homoepitaxial growth of Au and Pt, can explain the anistropic island shape. However, the straight edges of the islands and the termination of the islands along the 'troughs' of the hex-reconstruction are difficult to explain by anisotropic diffusion alone. Such a peculiar island shape (i.e., with straight edges and an island termination defined by the substrate) implies that Ag adatoms are less likely to attach themselves to the edges of the islands as long the underlying substrate is reconstructed. This can be rationalized by stronger Ag–Pt bonding on the unreconstructed-(1×1) surface than on the hex-reconstructed surface, which in turn can be viewed as the driving force responsible for lifting of the reconstruction underneath of Ag adislands. Furthermore, the island shape implies that an island lifts the reconstruction across the full width of a hex-unit cell. Once the reconstruction is lifted, further growth of the island is fast along the rows (because this does not require a new nucleation event) and this growth proceeds with the full width of a hex-unit cell. The observation that the reconstruction is lifted in a row-like fashion implies that the reconstruction is only stable if it exists across the full width of the unit cell. Partial removal of the hex-reconstruction appears to destabilize it and the structure reverts to the (1 0 0)-(1×1) arrangement over to the next 'trough'. It is intuitive that the 'trough' atoms have a lower energy than the 'ridge' atoms in the reconstruction. Thus the trough sites appear to stabilize the reconstruction for each row. As a consequence, the lifting of the reconstruction needs to be nucleated anew for each row, but once nucleated an island can grow along the row by adatom attachment. Furthermore, the strongly

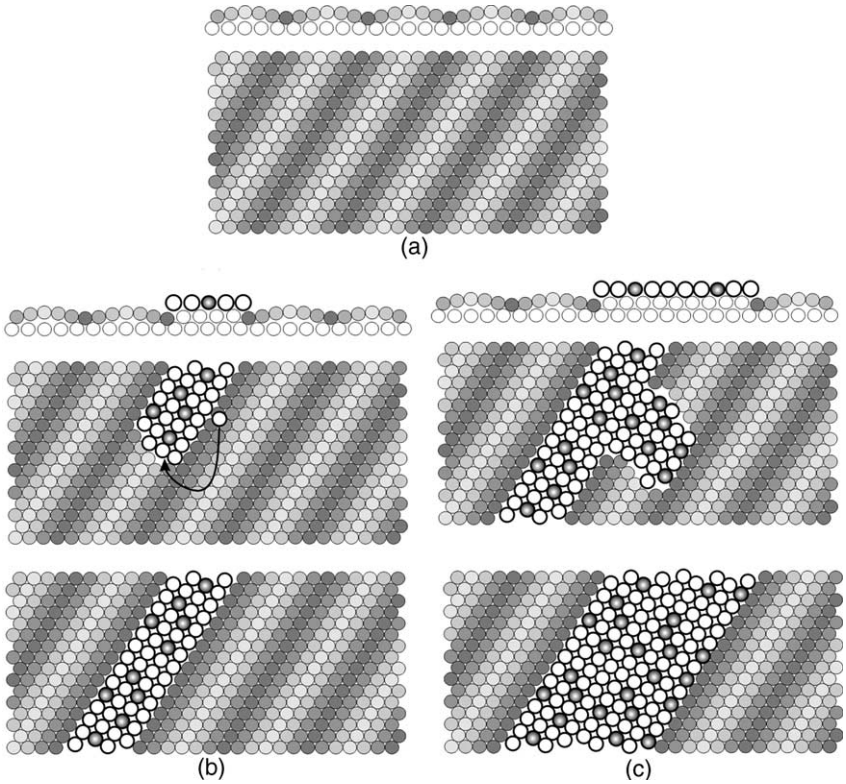

Fig. 2. Schematic illustration of the growth of an adisland on a Pt-hex surface. (a) Illustration of the hex-reconstructed surface. The gray shades indicate different vertical positions in the hex-overlayer. Bright circles correspond to atoms close to atop sites and dark circles reflect atoms close to fourfold hollow sites. (b) Ag deposition results in lifting of the reconstruction and nucleation of adislands across the full width of the periodicity of the reconstruction. Newly arriving Ag atoms (represented by open circles) can diffuse to the end of the adislands and continue growth of the island along the direction of the rows of the reconstruction. Pt atoms that are expelled out of the reconstruction and form an intermetallic alloy in the adisland are represented by gray-shaded circles. (c) Growth normal to the reconstruction-row pattern proceeds by a nucleation event that lifts the reconstruction across the full width of the adjacent unit cell. Subsequent island growth extend along the adjacent new 'row'.

anisotropic shape of the adislands implies that more than one Ag adatom is necessary to nucleate the lifting of the reconstruction. This is quite reasonable because the increase in the surface energy caused by lifting the reconstruction across the full width of a row has to be compensated by some energy gain due to the termination of the surface by Ag (Ag has about one-half of the surface energy of Pt [23]) and/or the increased bond-strength for Ag growing on a (1 0 0)-(1×1) substrate rather than on a hex-reconstructed substrate. Therefore, it could be anticipated that the critical Ag-cluster size required for nucleation would be larger than one, as required by the energy needed to compensate for the energy increase due to lifting of the reconstruction.

The growth of Ag on Pt(1 0 0)-hex has similarities to what was observed previously for the lifting of this reconstruction by exposure to CO molecules. In that case, the reconstruction is lifted in a row-by-row fashion, with much faster lifting along the rows compared to the direction normal to the rows [13]. For CO adsorption on Pt(1 0 0)-hex, it was determined that 4–5 CO molecules were necessary to nucleate the lifting of the reconstruction which involves 8–10 Pt substrate atoms [14].

In summary, we conclude that the anisotropic island shape with straight island edges is due to an

anisotropic stability of the hex-reconstruction of the substrate that always results in the lifting of the reconstruction across the full width of the unit cell describing the reconstruction. Once islands are nucleated, they grow relatively easily along the rows of the reconstruction. Anisotropic diffusion of adatoms along diffusion channels parallel to the adislands may enhance their anistropic shape. If these diffusion channels, defined by the reconstruction of the substrate, are too far away from the edges of the adislands lateral sticking of adatoms to the islands is prevented. At the end of the island adatoms can diffuse into an adjacent channel, which allows sticking to the end of the adisland and thus is promoting an elongated island shape. A similar behavior was for example discussed for Cu/Pd(1 1 0) [24].

3.2. Surface evolution with annealing temperature

In this subsection we present observations of the change in surface morphology and composition if an Ag deposit is annealed to higher temperatures. The surface morphology is characterized by room temperature STM studies after the sample was re-cooled from the annealing temperature to 300 K. Monitoring the Ag-AES signal while the sample temperature is varied and/or after some elapsed time at a constant, high temperature allows for a qualitative description of changes in the surface composition. The STM and AES studies are presented and discussed separately below.

3.2.1. STM

Annealing of submonolayer-Ag deposits on the Pt(1 0 0)-hex surface to 600 K for 10 s results in a change of the surface morphology compared to that obtained following deposition. STM images characterizing such annealed surfaces are displayed in Fig. 3. The islands are still clearly visible, however, the island edges are no longer as straight as they were after room temperature growth. Inspection of the 'substrate' adjacent to the island edges shows that the characteristic row structure of the hex-reconstruction has retreated from the island edges. Instead, the substrate that is located in the proximity of the islands exhibits a morphology that is similar to that of the islands themselves. The islands have also changed their appearance. Now, the islands exhibit a nanophasic structure of darker and brighter domains that can be identified as Pt and Ag regions, respectively. These domains exhibit an elongated and meandering structure. The nanophasic structure observed here is similar to that in Ag/Pt(1 1 1) studies where Ag alloys with Pt upon annealing to above 650 K and forms either a droplet or stripe domain pattern depending on the Ag coverage [17]. These nanophasic domains can be explained as stress domains that are a result of a competition between short-range attractive forces due to stronger

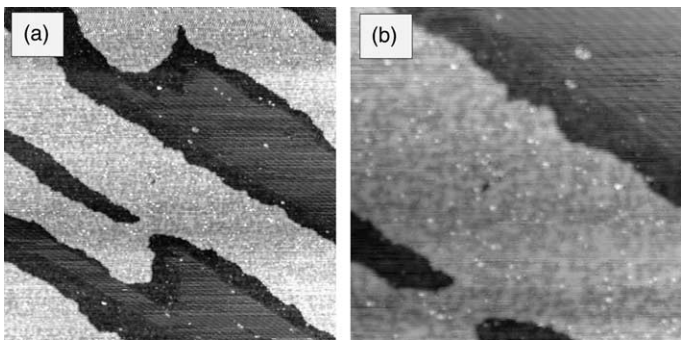

Fig. 3. STM images of a submonolayer-Ag deposit on Pt(1 0 0) after annealing to 600 K. (a) Scan area (110 nm)^2 and (b) scan area (45 nm)^2. The darker (Pt) and brighter (Ag) areas in the island structure have clustered together to form a nanophasic, intermixed Ag–Pt alloy. This nanophasic morphology has spread to the lower terraces and replaced the Pt(1 0 0)-hex-reconstruction in the vicinity of the adislands.

Ag–Ag bonding than Pt–Pt bonding, i.e. a positive exchange energy, and long-range repulsive forces mediated by stress-fields that arise because of the lattice-size mismatch between Ag and Pt.

Heating the Pt(1 0 0)-hex surface containing submonolayer-Ag deposits to 600 K causes the concentration of darker, i.e. Pt, regions in the islands to increase compared to that in the adislands grown at room temperature. This indicates that Pt from the substrate was incorporated into the islands and/or Ag was lost from the islands during heating. This and the observation that the hex-reconstruction has retreated from the island edges suggests that Ag from the islands has spread away from the islands and alloyed with the Pt in the region near the island. The Pt that is expelled by removal of the hex-reconstruction and incorporation of Ag to form an alloy, replaces the Ag atoms lost from the islands. This mechanism is represented schematically in Fig. 4. If the exchange of Ag and Pt between the islands and the substrate occurred in a one-to-one ratio, then the size of the adislands would not be expected to change. However, because the hex-reconstructed surface is more densely packed, alloying and lifting of the reconstruction results in 20% more Pt atoms being expelled out of the surface layer than are replaced by Ag. Thus, it could be expected that either (i) the adislands grow in size by 20%, (ii) additional pure-Pt adislands form, or (iii) Pt diffuses to step edges. Pure-Pt adislands were never observed. Neither of the other two possibilities are observable with STM in our studies since we cannot monitor the same surface area before and after annealing and thus cannot judge whether or not there has been a change in either the island size or terrace width. We believe that the former is unlikely because an increase in the island size would involve the overgrowth of the nanophasic Ag–Pt alloy-structure that surrounds the edges of the islands and we argue below that such a two-layer alloy is not favorable.

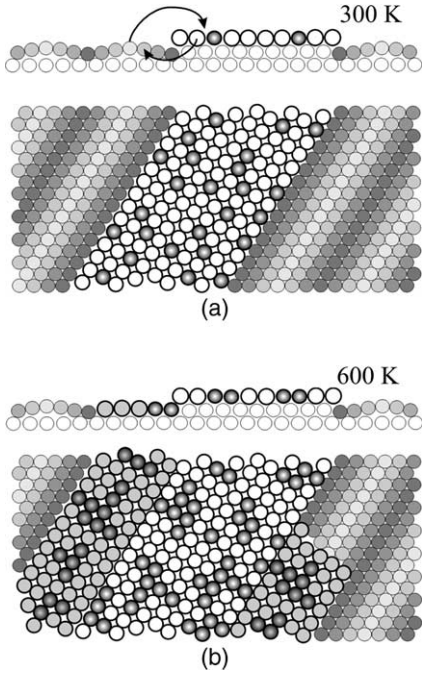

Fig. 4. Schematic illustration of spreading of the alloyed region upon annealing the sample. (a) Illustration of the island structure after growth at 300 K. (b) Ag atoms from the adislands can exchange places with Pt atoms in the lower terrace at 600 K and this results in a spreading of the alloyed region to the lower terrace.

Fig. 5(a) shows an image from a sample with 0.5-ML Ag that has been annealed to 600 K. Fig. 5(b) show an image from a similar sample with 0.4-ML Ag that was annealed to 900 K. From these large-scale STM images it is apparent that the surface morphology has also changed on this length scale compared to clean Pt(1 0 0). Step-bunches, rather than monatomic steps, primarily separate the flat terraces that were several hundreds of nm wide on the clean Pt(1 0 0)-hex surface. However, the surfaces shown in Fig. 5 exhibit depressions that often have an elongated shape and are separated by monatomic steps. This is surprising because such high temperature annealing usually results in flat terraces without holes that expose second-layer terraces.

We explain the shape of these structures as a consequence of the spreading and alloying of Ag from the adislands described above. Although Ag from the adislands is 'used up' to form an alloy on the Pt terraces, the adislands do not decrease in size, because Ag atoms from the islands are replaced by Pt that was expelled out of the 'substrate' upon alloy formation. This exchange between Ag and Pt continues until the composition is uniform across the surface. The reason why the

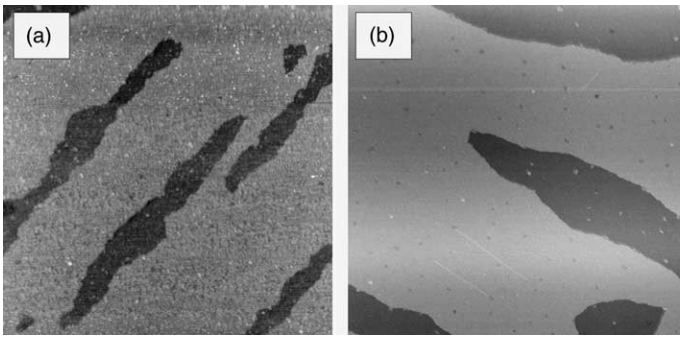

Fig. 5. STM images of (a) 0.5-ML Ag on Pt(1 0 0) annealed to 600 K. Scan area (120 nm)^2. (b) 0.4-ML Ag on Pt(1 0 0) annealed to 900 K. Scan area (300 nm)^2.

islands (or holes) do not coalesce upon annealing to 900 K is a consequence of the confinement of the alloy to the surface layer. This constraint, forces the coalescence of holes in the terraces to occur by interlayer mass transport. Interlayer-atom exchange is much slower and more highly activated then intralayer exchange or diffusion. Thus, the diffusion process appears to be too slow to allow for a complete coalescence of the holes during annealing to 900 K for 10 s.

3.2.2. AES

The influence of temperature was investigated by AES for samples with two different initial Ag coverages. The Ag(351,356) peak-to-peak AES intensity was monitored and plotted either against elapsed time after reaching a certain high temperature or against the temperature for constant heating rates. Fig. 6(a) and (b) show the evolution of the Ag AES intensity for an increase in the sample temperature with a constant heating rate of ~1 K/s. In Fig. 6(a), a film with a Ag coverage of 0.3 ML was heated to ~850 K and cooled down with an initial cooling rate of −1 K/s. No significant change in the Ag AES signal was observed for this film during heating or cooling. For a 1-ML Ag film, the situation is different as shown in Fig. 6(b). In this case, the Ag signal decreases with increasing temperature. The Ag intensity decreased by 10% from its initial value at 300 K after heating to 850 K for a constant heating rate of 1 K/s. If the sample was immediately cooled after reaching 850 K with a constant cooling rate, the Ag intensity kept decreasing for a small temperature range but then started to increase again. The slope of the increasing Ag signal versus temperature is about the same as the slope during heating. The initial continuing decrease in the Ag signal after starting the cool-down process results in a small hysteresis and therefore the Ag intensity did not follow the same trace as during heating.

Experiments in which samples with 1-ML Ag were heated rapidly to a target temperature and then kept constant at this value are shown in Fig. 6(c) and (d). In Fig. 6(c), the sample was heated to 600 K and then kept constant at this temperature for 950 s. The Ag AES intensity remained unchanged during this time. Subsequent heating to 800 K resulted in a decrease in the Ag signal. Keeping the temperature constant at this value causes a further decrease in the Ag signal. This can be observed more clearly in Fig. 6(d) where the sample was heated rapidly to 800 K and then held at this temperature for 1000 s. The Ag signal continuously decreased during this time. Cooling the sample resulted again in an increase in the Ag signal.

TPD experiments show that no Ag desorbs from the surface below 900 K [21]. Thus, a decrease in the Ag-AES signal can only be explained by Ag clustering (3D-island formation) at the surface or Ag diffusion into the crystal. No evidence for clustering of Ag has been found in STM studies and the much lower surface energy of Ag compared to Pt [23] is expected to favor a wetting of the surface at all temperatures. Thus, we

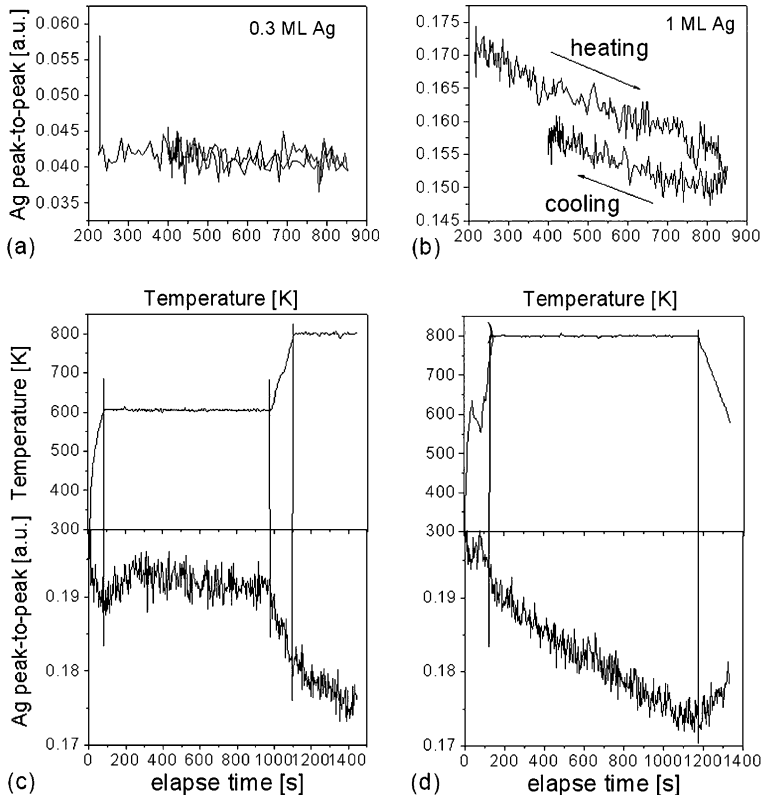

Fig. 6. Temperature-dependent AES intensities measured for (a) 0.3-ML Ag and (b) 1-ML Ag during heating at a constant rate of 1 K/s and cooling with an initial rate of 1 K/s. (c) and (d) show AES intensities measured on samples with 1-ML Ag coverage as a function of elapsed time at different temperatures. The upper graphs show the sample temperature versus time and the lower graphs show the Ag peak-to-peak AES intensities during the same time.

propose that the decrease in the Ag-AES signal is a result of some mixing of Ag with the second and bulk layers of the crystal at elevated temperatures. For low initial Ag coverages, no significant change in the AES signal was observed, indicating that there is no substantial Ag diffusion into the subsurface region even at elevated temperatures. For 1-ML Ag coverage, the Ag-AES signal was temperature dependent and changed almost reversibly with heating and cooling of the sample. This and the faster diffusion at 800 K compared to 600 K can be explained by proposing two processes. We propose that Ag and Pt in the first and second layers can undergo place exchange at relatively low temperatures, and this may be a fast process so that the surface adjusts to a new equilibrium composition quickly after a temperature change and does not change significantly with time if the temperature is constant. This process is reversible upon cooling of the sample. Annealing to higher temperatures (e.g., 800 K) allows for diffusion deeper into the bulk or accelerates it to a measurable value. This is a slower process with a higher activation barrier. Continuous loss of Ag into the bulk explains the continuous decrease of the Ag-AES signal at 800 K. A small loss of Ag by diffusion into the bulk at 850 K also explains the observed hysteresis in the heating and cooling cycle displayed in Fig. 6(b).

Intermixing of Ag and Pt appears to be unfavorable because it was previously claimed that Ag and Pt possesses a positive exchange energy and Ag has a lower surface energy. However, the entropic contribution to the free energy may drive limited

mixing and disordering of the surface. One can argue that Ag and Pt can sufficiently disorder in the surface layer to increase configurational entropy at low Ag coverages and therefore no significant change in the AES signal was observed on such samples (Fig. 6(a)). For a pseudomorphic Ag-monolayer, on the other hand, intermixing of Ag and Pt between the surface layer and the Pt substrate has to occur to increase configurational disorder in the surface layer. Consequently, Ag diffuses into the subsurface region of the Pt crystal and the Ag AES-signal decreases with increasing temperature. This process is reversible and upon cooling Ag diffuses back to the surface as the entropy contribution to the free energy becomes less dominant and the free energy of the system is reduced by increasing the amount of Ag at the surface.

4. Summary

Initial Ag growth on Pt(1 0 0)-hex at 300 K is strongly influenced by the surface reconstruction of the Pt crystal. Adisland-growth proceeds in elongated structures along the rows of the hex-reconstruction. We explain this growth mode by an anisotropic stability of the hex-reconstruction. Such formation of elongated islands has been previously reported after the deposition of several metals on this surface and this behavior may be expected on (1 0 0) hex-reconstructed surfaces, i.e. Pt, Au, and Ir, for a variety of deposited materials. Annealing of the adisland structure above 600 K results in the formation of a nanophasic Ag–Pt alloy. The alloy formation starts at the perimeter of the adislands and spreads across the surface by exchanging Ag from the adislands with Pt from the adjacent lower terraces. The diffusion of Ag is limited to the surface layer. This confinement of Ag to the surface kinetically restricts the coalescence of alloy terraces. Although the nanophasic alloy remains essentially confined to the surface layer, AES indicates limited dissolution of Ag into bulk Pt after prolonged heating at elevated temperatures. Two processes for Ag diffusion are proposed to explain the temporal response of the AES signal upon changing the sample temperature: (i) Site exchange between Ag and Pt in the first and second layer, respectively, and (ii) vacancy mediated bulk diffusion processes of Ag in the subsurface region. The former is a fast, reversible process observed at all of the temperatures studied in this work. This process appears to be mainly entropy driven. Increasing configurational disorder (mixing) at elevated temperatures reduces the free energy of the system and upon cooling a lowering of the free energy by increasing the Ag content in the surface layer is obtained. The latter process is more highly activated and can only be observed at temperatures higher than 700 K on the time-scale of these experiments.

Acknowledgements

This work was partially supported by the Analytical and Surface Chemistry Program in the Division of Chemistry, National Science Foundation (NSF).

References

[1] S. Hagstrom, H.B. Lyon, G. Samorjai, Phys. Rev. Lett. 15 (1965) 491.
[2] G. Ritz, M. Schmid, P. Varga, A. Borg, M. Rønning, Phys. Rev. B 56 (1997) 10518.
[3] D.L. Albernathy, S.G.J. Mochrie, D.M. Zehner, G. Grübel, D. Gibbs, Phys. Rev. B 45 (1992) 9272.
[4] Y.Y. Yeo, C.E. Wartnaby, D.A. King, Science 268 (1995) 1731.
[5] S. Günther, E. Kopatzki, M.C. Bartelt, J.W. Evans, R.J. Behm, Phys. Rev. Lett. 73 (1994) 553.
[6] R.Q. Hwang, C. Günther, J. Schröder, S. Günther, E. Kopatzki, R.J. Behm, J. Vac. Sci. Technol. A 10 (1992) 1970.
[7] T.R. Linderoth, J.J. Mortens, K.W. Jacobsen, E. Lægsgaard, I. Stensgaard, F. Besenbacher, Phys. Rev. Lett. 77 (1996) 87.
[8] H.J. Venvik, C. Berg, A. Borg, S. Raan, Phys. Rev. B 53 (1996) 16587.
[9] A. Ramstad, F. Strisland, S. Raaen, T. Worren, A. Borg, C. Berg, Surf. Sci. 57 (1999) 25.
[10] M. Batzill, B.E. Koel, in preparation.
[11] C. Berg, H.J. Venvik, F. Strisland, A. Ramstad, A. Borg, Surf. Sci. 409 (1998) 1.
[12] G. Gilarowski, J. Mendez, H. Niehus, Surf. Sci. 448 (2000) 290.
[13] A. Borg, A.-M. Hilmen, E. Bergene, Surf. Sci. 306 (1994) 10.
[14] A. Hopkinson, J.M. Bradley, X.-C. Guo, D.A. King, Phys. Rev. Lett. 71 (1993) 1597.

[15] H. Brune, G. Bales, J. Jacobsen, C. Boragno, K. Kern, Phys. Rev. B 60 (1999) 5991.
[16] H. Röder, R. Schuster, H. Brune, K. Kern, Phys. Rev. Lett. 71 (1993) 2086.
[17] P. Zeppenfeld, M.A. Krzyzowski, Ch. Romainczyk, R. David, G. Comsa, H. Röder, K. Bromann, H. Brune, K. Kern, Surf. Sci. 342 (1995) L1131.
[18] J.S. Tsay, Y.D. Yao, C.S. Shern, Phys. Rev. B 58 (1998) 3609.
[19] J. Tersoff, Phys. Rev. Lett. 74 (1995) 434.
[20] M. Batzill, B.E. Koel, Surf. Sci. Lett. 498 (2002) L85.
[21] M. Batzill, B.E. Koel, Europhys. Lett. 64 (2003) 70.
[22] D. Beck, M. Batzill, C. Baur, B.E. Koel, Rev. Sci. Instrum. 73 (2002) 1267.
[23] A.R. Miedema, Z. MetaIlkd. 69 (1978) 287.
[24] Y. Li, M.C. Bartelt, J.W. Evans, N. Waechli, E. Kampshoff, K. Kern, Phys. Rev. B 56 (1997) 12539.